

1 **Title**

2 Biuret toxicity induces accumulation of nitrogen-rich compounds in rice plants

3

4 **Authors' names and affiliations**

5 Kumiko Ochiai<sup>1</sup>, Yosuke Nomura<sup>1</sup>, Asuka Uesugi<sup>1</sup>, and Toru Matoh<sup>1,2</sup>

6 Kumiko Ochiai and Yosuke Nomura equally contributed to this work.

7 <sup>1</sup>Graduate School of Agriculture, Kyoto University, Kyoto 606-8502 Japan

8 <sup>2</sup>Kyoto Agriculture Research Institute (Kyoto Nogyo no Kenkyusho), Kyoto 606-8032 Japan

9

10 **\*To whom correspondence should be addressed**

11 Kumiko Ochiai, Laboratory of Plant Nutrition, Division of Applied Life Sciences, Graduate

12 School of Agriculture, Kyoto University, Kyoto 606–8502 Japan

13 Email: ochiai.kumiko.7m@kyoto-u.ac.jp

14

15 **ORCID**

16 Kumiko Ohiai, <https://orcid.org/0000-0001-9137-200X>

17 Asuka Uesugi, <https://orcid.org/0000-0003-1698-4289>

18 Toru Matoh, <https://orcid.org/0000-0002-8418-2328>

19

20 **Abstract**

21 Aims

22 Excess biuret, a common impurity in urea fertilizers, is toxic to plants. Little is known about the  
23 mechanisms of biuret toxicity in plants. This study aimed to investigate the accumulation of biuret  
24 and the changes in metabolites in rice (*Oryza sativa*) plants under biuret toxicity.

25 Methods

26 A previous study had shown that transgenic rice plants overexpressing bacterial *biuret hydrolase*  
27 had improved biuret tolerance. Here, we grew wild-type and bacterial *biuret hydrolase*-  
28 overexpressing rice plants in hydroponics at different biuret levels. Concentrations of biuret and  
29 allantoin, a nitrogenous intermediate in the purine degradation pathway, in the plants were  
30 determined. The expression levels of genes related to purine degradation and ureide metabolisms  
31 were analyzed using wild-type plants. Additionally, we performed a metabolome analysis using  
32 rice suspension cells.

33 Results

34 The *biuret hydrolase*-overexpressing plants did not contain biuret, whereas wild-type plants  
35 accumulated biuret in shoots in the order of mmol L<sup>-1</sup> tissue water. The concentration of allantoin  
36 in shoots of wild-type plants under biuret toxicity was higher than those in control conditions.  
37 Inhibition of allantoinase activity by biuret was not detected, and allantoin accumulation appeared  
38 to be associated with changes in the expression of *allantoinase*, *allantoate amidohydrolase* and  
39 putative allantoin transporter genes. Furthermore, another nitrogenous compound citrulline,  
40 which is a non-protein amino acid, accumulated in rice suspension cells under biuret toxicity.

41 Conclusion

42 The accumulation of these compounds suggests that rice plants subjected to biuret toxicity need  
43 to reduce the concentration of surplus ammonium ions via synthesizing nitrogen-rich compounds.

44

45 **Key words: allantoin, biuret, citrulline, nitrogen, rice**

46 **Introduction**

47 Biuret is a common impurity in urea fertilizers. It is a byproduct of the urea granulation process  
48 and is formed by the thermal condensation of two urea molecules. When urea fertilizers are  
49 added to arable lands, biuret, a contaminant in these fertilizers, is also applied. Biuret in the soil  
50 is decomposed by microorganisms and eventually produces ammonia and carbon dioxide, albeit  
51 more slowly than urea does (Aukema et al., 2020; Cameron et al., 2011; Robinson et al., 2018).  
52 Biuret is not known to be toxic to animals; however, excess biuret can stunt plant growth and  
53 cause chlorosis of leaves (Mikkelsen, 1990). Consequently, the permissible biuret concentration  
54 in many countries is 1.2% for urea fertilizers.

55 Previous studies on biuret toxicity have shown that it inhibits protein synthesis in plants (Ogata  
56 and Yamamoto, 1959; Webster et al., 1957). A recent experiment also found that biuret toxicity  
57 can alter the expression levels of many genes involved in environmental stress response (Ochiai  
58 et al., 2020). However, the mechanisms underlying biuret toxicity are still not well understood.  
59 Clarification of this mechanism may help prevent potential plant injury caused by biuret as the  
60 impurity in urea fertilizers.

61 We previously found that rice plants overexpressing *biuret hydrolase* from a soil bacterium had  
62 an enhanced biuret tolerance (Ochiai et al., 2020). The experiment used <sup>15</sup>N-labeled biuret and  
63 showed that *biuret hydrolase*-overexpressing plants take up more biuret than wild-type plants.  
64 However, the form of <sup>15</sup>N in plants after uptake is not known. In this study, we examined the  
65 biuret accumulation, in wild-type and *biuret hydrolase*-overexpressing rice plants using HPLC-  
66 UV, to understand how the biuret accumulation in plants causes injury. Plants grown with 0.3  
67 mmol L<sup>-1</sup> biuret showed stress symptoms and accumulated biuret in the shoots. The  
68 overexpression of *biuret hydrolase* led to biuret consumption and stress alleviation.

69 In addition, we hypothesized that biuret inhibits the metabolism of compounds with a similar  
70 structure, specifically ureide compounds, in a competitive manner. Among ureide, we focused  
71 on allantoin because of its multiple roles and importance to plants. Allantoin, a compound  
72 composed of a hydantoin ring and ureido group, is an intermediate in the purine degradation  
73 pathway. It contains four nitrogen (N) atoms per molecule and contributes to N recycling in  
74 plants (Soltabayeva et al., 2018). Allantoin and allantoic acid are the dominant forms of  
75 assimilated-N transported from roots to shoots through the xylem in tropical leguminous plants  
76 (Schubert et al., 1986). Additionally, many plant species accumulate allantoin under abiotic  
77 stress such as salinity, drought, and heavy metal toxicity (Casartelli et al., 2019; Kaur et al.,  
78 2021; Lescano et al., 2016; Nourimand and Todd, 2016; Watanabe et al., 2013). The  
79 accumulated allantoin can enhance the abiotic stress tolerance of plants (Watanabe et al., 2013).  
80 We examined whether biuret disrupted allantoin metabolism and found that allantoin  
81 accumulated in biuret-treated rice shoots. However, contrary to our expectations, biuret did not  
82 show competitive inhibition of the allantoin-degrading enzyme; therefore, we further  
83 investigated the mechanism of allantoin accumulation.

84 Furthermore, in addition to the analysis targeting allantoin metabolism, we took a  
85 comprehensive approach to examine metabolic processes affected by biuret toxicity. Concretely,  
86 we performed a metabolome analysis using rice suspension cells and showed a citrulline  
87 accumulation in cells under biuret toxicity.

88

## 89 **Materials and methods**

### 90 **Plant materials and growth conditions**

91 Seeds of *japonica* rice (*Oryza sativa*) cultivar Nipponbare were purchased from Nouken (Kyoto,  
92 Japan). Transgenic rice lines overexpressing bacterial *biuret hydrolase* were developed from

93 Nipponbare (Ochiai et al., 2020), and the T<sub>3</sub> generation was used in this study. Seeds of rice  
94 were soaked in distilled water added with fungicide (Trifumin; Nippon Soda, Tokyo, Japan) for  
95 two days. Ten seeds were sown on a mesh (18 mesh, 23 x 34 mm) stretched on a plastic slide  
96 mount and floated on a culture solution. The culture solution contained 1 mmol L<sup>-1</sup> (NH<sub>4</sub>)<sub>2</sub>SO<sub>4</sub>,  
97 0.5 mmol L<sup>-1</sup> KCl, 0.25 mmol L<sup>-1</sup> KH<sub>2</sub>PO<sub>4</sub>, 0.5 mmol L<sup>-1</sup> CaCl<sub>2</sub>, 0.5 mmol L<sup>-1</sup> MgCl<sub>2</sub>, and  
98 Arnon's micronutrient (cited by Hewitt, 1966). Iron was supplied at the rate of 5 mg Fe L<sup>-1</sup> as  
99 ethylenediamine-*N,N,N',N'*-tetraacetic acid iron(III) sodium salt. Biuret was added to the  
100 solution at the desired concentration whenever necessary. The culture solution was prepared  
101 with tap water and not aerated. At most, six nets were floated in a 1-L plastic container. Plants  
102 were raised in a growth chamber (NS-280 FHW; Takayama Seisakusyo, Kyoto, Japan) under  
103 the following conditions: temperature, 30°C; photoperiod, 12 h; and light intensity, 350 μmol m<sup>-2</sup>  
104 s<sup>-1</sup>.

105 The rice Oc cell suspension culture line (Baba et al., 1986) was provided by RIKEN BRC,  
106 participating in the National BioResource Project of the MEXT/AMED, Japan. The cells were  
107 maintained as described by Ochiai et al. (2020).

108

### 109 **Confirmation of transgene in *biuret hydrolase*-overexpressing rice plants**

110 DNA was extracted from the second leaves of individual T<sub>3</sub> plants of *biuret hydrolase*-  
111 overexpressing lines, B3-9-1 and B2-3-3 (Ochiai et al., 2020). Second leaves were also excised  
112 from the wild-type plants to equalize the effects of leaf clipping. The transgene was detected by  
113 PCR using the primers 5'-ATGAAGACACTTTCCAGCGC-3' and 5'-  
114 TGGCAAATGCCTCTCAAGG-3' and Blend Taq polymerase (Toyobo, Osaka, Japan). Plants  
115 confirmed to possess *biuret hydrolase* were used in the analysis.

116

117 **Determination of biuret and allantoin in rice seedlings**

118 At harvest, the rice roots were rinsed for 3 mins, three times with 100 mL of distilled water.  
119 Several seedlings were combined into a single sample, blotted and dried with paper towels,  
120 separated into shoots and roots, weighed, and freeze-dried. After determining the dry weights,  
121 the samples were ground into a powder using a ball mill.  
122 About 10 mg of the powdered sample were resuspended in 250  $\mu\text{L}$  of distilled water. After  
123 centrifugation, a 35  $\mu\text{L}$  aliquot of the supernatant was mixed with 465  $\mu\text{L}$  of acetonitrile and  
124 centrifuged again. A 20  $\mu\text{L}$  aliquot of the supernatant was injected into the HPLC system (LC-  
125 10AS; UV detector: SPD-10A, Shimadzu, Kyoto, Japan) equipped with a hydrophilic  
126 interaction chromatography (HILIC) column (YMC-Triart Diol-HILIC, 5  $\mu\text{m}$ , 4.6 x 250 mm,  
127 YMC Co. Ltd., Kyoto, Japan). The isocratic eluent was a mixture of 930 mL of HPLC-grade  
128 acetonitrile and 70 mL of distilled water. In some experiments, we modified the eluent to a  
129 mixture of 940 mL of acetonitrile and 60 mL of distilled water to improve the separation. In this  
130 case, a 94:6 mixing ratio was used for sample preparation. Elution was performed at a flow rate  
131 of 0.5 mL  $\text{min}^{-1}$ , and the effluent was monitored at 190 nm. The colorimetric determination of  
132 allantoin was performed as described by Young and Conway (1942). The allantoin  
133 concentration in rice plants determined by HPLC was consistent with that measured by the  
134 colorimetric method (Supplemental Fig. S1).

135

136 **Determination of total-N**

137 The total-N in the plant samples was determined by the combustion method using an NC  
138 analyzer (Sumigraph NC-22F, Sumika Chemical Analysis Service, Osaka, Japan).

139

140 **Determination of free amino acids**

141 Free amino acids were extracted from freeze-dried plant powder with 80% ethanol at 80°C for  
142 20 min. The concentration of amino acids in the extract was determined by the ninhydrin  
143 method (Moore and Stein, 1954) using leucine as a standard.

144

#### 145 **Inhibition assay for allantoinase activity**

146 Allantoinase activity was assayed according to Duran and Todd (2012). Shoots of 9-day-old  
147 Nipponbare seedlings grown without biuret were weighed and homogenized with a five-fold  
148 volume of extraction buffer containing 50 mmol L<sup>-1</sup> Tricine (pH 8.0) and 2 mmol L<sup>-1</sup> MnSO<sub>4</sub>.  
149 After centrifugation, the supernatant was used in the inhibition assay. The enzymatic reaction  
150 was initiated by the addition of allantoin as a substrate at a final concentration of 10 mmol L<sup>-1</sup> to  
151 the supernatant. Biuret at final concentration of 0, 0.5, and 5 mmol L<sup>-1</sup> was added to the reaction  
152 mixture together with the allantoin. The total volume of the reaction mixture was 0.5 mL. The  
153 reaction mixture was incubated at 30°C for 30 min, and the reaction was stopped by adding 0.25  
154 mL of 0.15 mol L<sup>-1</sup> HCl. Allantoic acid in the reaction mixture was colorimetrically determined  
155 (Young and Conway, 1942). The allantoic acid content of the crude extract was also determined  
156 and subtracted.

157 Protein concentrations in the crude extracts were determined by the Bradford method using  
158 Protein Assay CBB Solution (Nacalai Tesque, Kyoto, Japan).

159

#### 160 **Gene expression analysis**

161 Rice plants were grown with and without 0.3 mmol L<sup>-1</sup> biuret supplementation in the culture  
162 solution. Four to seven-day-old seedlings were harvested during the light period. Two to four  
163 plants were combined into a single sample. Experiments were repeated twice. Total RNA was  
164 extracted from roots and shoots using the Plant Total RNA Extraction Miniprep System



165 (Viogene, Taipei, Taiwan). First-strand cDNA was synthesized from total RNA using oligo dT  
166 primers and ReverTra Ace polymerase (Toyobo, Osaka, Japan). Quantitative real-time RT-PCR  
167 was performed using the TP850 Thermal Cycler Dice Real Time System Single (Takara Bio,  
168 Shiga, Japan) and THUNDERBIRD SYBR qPCR MIX (Toyobo, Osaka, Japan). Primer pairs  
169 used for target genes were 5'-CTGGAGCGTGCTATGTTTCA-3' and 5'-  
170 AGCTTGTGGACCACCAAAC-3' for *xanthine oxidase*, 5'-  
171 TCAGCTAAGGATGCCGAACC-3' and 5'-ATGGTCCCCTGTGGTTCATC-3' for *urate*  
172 *oxidase*, 5'-TAACGTCGCTCCTGGTTTCT-3' and 5'-ACAGAGGGACATGGAAATGC-3'  
173 for *allantoin synthase*, 5'-AACGCATACCCGATGTTTCAG-3' and 5'-  
174 TGTCTTTCATCGCACGTTGC-3' for *allantoinase*, 5'-TCTGACAAGAGTGGCACGAC-3'  
175 and 5'-GACAGGCCCTTGTTCATGT-3' for *allantoate amidohydrolase*, 5'-  
176 TATTCAGCCCTTTCCTGAC-3' and 5'-GGTGGTAGGGCTGATTTTGA-3' for  
177 *ureidoglycine aminohydrolase*, 5'-TCGCATGTGGAAATTGATGT-3' and 5'-  
178 ATAATAGCACGCCACGGTTC-3' for *ureidoglycolate amidohydrolase*, 5'-  
179 TGAACCACAGCAACACCAAT-3' and 5'-GCCACTTCAGGCTCTTGTTTC-3' for *ureide*  
180 *permease 1*, 5'-CTCTGCTGTACATGCCTCCA-3' and 5'-TGTTTGGTTCCACACTTCCA-3'  
181 for *ureide permease 2*, 5'-GAGAAGAGGCGATCCATCAA-3' and 5'-  
182 CGAGAAGAGGGAGAAGCAGA-3 for *ureide permease 3*. The expression levels of the genes  
183 were normalized to the mean expression level of *Ubiquitin* (primer pairs: 5'-  
184 AGAAGGAGTCCACCCTCCACC-3' and 5'-GCATCCAGCACAGTAAAACACG-3'; Yamaji  
185 and Ma, 2009) and *Actin 1* (primer pairs: 5'-ATCCTTGTATGCTAGCGGTCTGA-3' and 5'-  
186 ATCCAACCGGAGGATAGCATG-3'; Caldana et al., 2007).

187

188 **Metabolome analysis in rice suspension cells**

189 Biuret treatment was initiated by subculturing 2 mL of seven-day-old cell suspension into 80  
190 mL of the medium supplemented with or without 0.3 mmol L<sup>-1</sup> biuret. Then, cells were  
191 harvested three and five days after subculturing. Cells were collected by suction filtration,  
192 rinsed with distilled water, frozen with liquid nitrogen, and stored at -80°C until analysis.  
193 Samples were prepared in duplicate.

194 Metabolomic analysis was done by the Kazusa DNA Research Institute, Kisarazu, Chiba, Japan.  
195 Briefly, rice cells were extracted with methanol. A 5-μL aliquot of the extract was analyzed  
196 using liquid chromatography-mass spectrometry (LC-MS). LC-MS analysis was conducted on  
197 an Agilent 1200 series LC system (Agilent Technologies, Santa Clara, CA, USA) equipped with  
198 a TSK-GEL ODS-100V column (5μm, 3 × 50 mm; Tosoh, Tokyo, Japan) and connected to an  
199 LTQ ORBITRAP XL mass spectrometer (Thermo Fisher Scientific, Waltham, MS, US). The  
200 gradient mobile phase consisted of 0.1% formic acid in water (solution A), and acetonitrile  
201 (solution B). MS detection was performed using positive-ion mode electrospray ionization. The  
202 data were converted into text files using the MSGet software  
203 (<http://www.kazusa.or.jp/komics/software/MSGet>) and then organized using the PowerGet  
204 software (Sakurai et al., 2014).

205 Peaks detected in both the replicates of at least one of the four sample groups were used for  
206 subsequent analysis. Statistical analyses were performed using the R software (R Core Team,  
207 Vienna, Austria). The peak intensities were log<sub>2</sub> transformed and then normalized to the median  
208 of each sample, and the missing values were replaced by half the value of the minimum peak  
209 intensity. The Welch's t-test was used to test the differences between the means of the two  
210 groups. The annotation information provided by Kazusa DNA Research Institute and a web  
211 program Metaboanalyst 5.0 (Pang et al., 2021) was used to identify candidate compounds for  
212 the peaks.

213

## 214 **Results**

### 215 **Biuret accumulation in rice seedlings**

216 First, biuret concentration was determined in 7-day-old rice (Nipponbare) seedlings grown with  
217 0, 0.1, and 0.3 mmol L<sup>-1</sup> biuret supplemented in the culture solution. Visual observation showed  
218 chlorosis on the leaves of plants under 0.3 mmol L<sup>-1</sup> biuret treatment (see Supplemental Figure  
219 S2 for the typical symptoms). The root and shoot dry weights were not significantly different  
220 among treatments. However, shoot dry weights tended to decrease with an increasing biuret  
221 concentration in the culture solution (Fig. 1a). Biuret concentration in roots and shoots increased  
222 as the biuret concentration in the culture solution increased (Fig. 1b). Consistent with our  
223 previous <sup>15</sup>N-labeled biuret uptake experiment (Ochiai et al., 2020), the biuret concentration in  
224 the shoots was higher than that in the roots, suggesting that biuret accumulated in the shoots  
225 with the transpirational volume flow.

226 The biuret concentration was also determined for 9-day-old transgenic rice lines overexpressing  
227 bacterial *biuret hydrolase* under the control of a modified CaMV35S promoter. The dry weight  
228 of the wild-type plants was significantly reduced by 0.3 mmol L<sup>-1</sup> biuret in the culture solution  
229 (Fig. 1d). In contrast, biuret injury was alleviated in the *biuret hydrolase*-overexpressing lines  
230 grown in the same container (Fig. 1d, Supplemental Fig. S2). Biuret was not detected in *biuret*  
231 *hydrolase*-overexpressing plants grown with 0.3 mmol L<sup>-1</sup> biuret (Fig. 1f). The results indicated  
232 that excess biuret in WT plants was the cause of biuret injury.

233

### 234 **Allantoin accumulation in rice seedlings**

235 The allantoin concentration in 7-day-old wild-type rice was higher in the roots than in the shoots  
236 (Fig. 1c). However, the allantoin concentration in roots did not differ among treatments. On the

237 other hand, the shoot allantoin concentration was significantly higher in plants under 0.3 mmol  
238 L<sup>-1</sup> biuret treatment than in control and 0.1 mmol L<sup>-1</sup> biuret-treated plants. The shoot total N  
239 concentrations were 51.7, 49.8, and 49.4 mg g<sup>-1</sup> dw for plants grown with 0, 0.1, and 0.3 mmol  
240 L<sup>-1</sup> biuret, and there was no significant difference among treatments ( $p < 0.05$ , Tukey's test).  
241 The shoot allantoin concentration of the 9-day-old *biuret hydrolase*-overexpressing plants under  
242 0.3 mmol L<sup>-1</sup> biuret toxicity was not different from that of the control (Fig. 1f). This indicated  
243 that there was no increase in allantoin accumulation in the absence of injury. The root allantoin  
244 concentration of biuret-treated plants was lower than that of the control in the wild-type and line  
245 B-2-3-3 plants (Fig. 1f).  
246 First, we examined whether biuret inhibited allantoin degradation enzyme, allantoinase (ALN),  
247 activity. In the assay using crude extracts prepared from shoots of rice seedlings grown without  
248 biuret and 5 mmol L<sup>-1</sup> allantoin as the substrate, biuret up to 5 mmol L<sup>-1</sup> did not inhibit the  
249 allantoic acid-producing activity of ALN (Fig. 2).  
250 The expression levels of genes relating to the allantoin synthesis and degradation were then  
251 analyzed to investigate the mechanism of allantoin accumulation. In the purine degradation  
252 pathway, the primary substrate xanthine is oxidized to uric acid by xanthine dehydrogenase  
253 (XDH). Uric acid is then oxidized to allantoin via 5-hydroxyisourate and 2-oxo-4-hydroxy-4-  
254 carboxy-5-ureidoimidazoline. These steps are catalyzed by two enzymes, uric acid oxidase  
255 (UOX) and bifunctional allantoin synthase (ALNS). Allantoin is then hydrolyzed to allantoic  
256 acid by ALN. The downstream hydrolysis reactions resulting in allantoic acid to ureidoglycine,  
257 ureidoglycine to ureidoglycolate, and ureidoglycolate to hydroxyglycine are catalyzed by  
258 allantoate amidohydrolase (AAH), ureidoglycine aminohydrolase (UGlyAH), and  
259 ureidoglycolate amidohydrolase (UAH), respectively.

260 The expression level of genes in the allantoin synthetic pathway, *OsXDH* (Os03g0429800),  
261 *OsUO* (Os01g0865100), and *OsALNS* (Os03g0390700), was mostly not changed by the 0.3  
262 mmol L<sup>-1</sup> biuret treatment in 4 to 7-day-old seedlings. However, there was a significant increase  
263 in the expression level of *OsXO* in the 7-day-old root and shoot (Fig. 3a-c). The expression level  
264 of *OsALN* (Os04g0680400) in 4 to 6-day old root decreased under the biuret treatments. On the  
265 other hand, the expression level in shoots did not differ between the treatments (Fig. 3d). The  
266 result of no difference in shoot *OsALN* expression was different from that of our preliminary  
267 study (Supplemental Fig. S3) but obtained by two independent trials (Fig. 3d). The expression  
268 level of *OsAAH* (Os06g0665500) in 5 and 6-day-old roots and 6, and 7-day-old shoots, and  
269 *OsUAH* (Os12g0597500) in 5-day-old roots showed significant decrease under the biuret  
270 treatment (Fig. 3, e and g). The expression level of *OsUGlyAH* (Os07g0495000) was not  
271 changed by the biuret treatment (Fig. 3f).

272 Additionally, the expression levels of the putative allantoin transporter gene *OsUPS1* (*ureide*  
273 *permease 1*, Os12g0503000) and the two homologous genes *OsUPS2* (Os12g0502800) and  
274 *OsUPS3* (Os12g0503300) were examined. The biuret treatment significantly increased the  
275 expression level of *OsUPS1* in the shoots of 5-to 7-day-old seedlings (Fig. 3h). The expression  
276 levels of *OsUPS2* in the roots of 4 and 5-day-old seedlings were significantly lower in plants  
277 grown with biuret than in control plants (Fig. 3i). The expression level of *OsUPS3* was  
278 relatively low compared with the other two homologs and did not differ between the treatments  
279 (Fig. 3j).

280 Consistently, allantoin concentration in 8-day-old seedlings that were grown together with  
281 plants used for gene expression analysis was significantly higher in shoots under biuret  
282 treatment than in the control plants (data on three of six samples are shown in Fig. 6b).  
283

284 **Metabolite changes in rice suspension cells under biuret toxicity**

285 Adding 0-1 mmol L<sup>-1</sup> biuret to the culture medium reduced the growth of suspension-cultured  
286 rice cells in a concentration-dependent manner (Ochiai et al., 2020). Under 0.3 mmol L<sup>-1</sup> biuret  
287 treatment, the cell fresh weight was significantly lower than control cells seven days after  
288 subculturing; however, the difference was not yet significant five days after subculturing  
289 (Ochiai et al., 2020).

290 We performed comprehensive metabolite analysis of suspension-cultured rice cells to  
291 investigate the changes in metabolome induced by biuret toxicity. Metabolites of rice  
292 suspension cells at two-time points, day 3 (d3) and day 5 (d5) after subculturing, for two  
293 treatments, biuret treatment supplied 0.3 mmol L<sup>-1</sup> biuret and a control treatment without biuret,  
294 were analyzed using LC-MS technique. Of the 3,566 peaks detected (Supplemental Data S1),  
295 993 peaks consistently detected in replicates of at least one of the four sample groups were used  
296 for subsequent analysis.

297 Principal component analysis was performed to compare the metabolite profiles of rice  
298 suspension cells. The first principal component (PC1) accounted for 25.3% of the total variance,  
299 the second (PC2) for 21.2%, and the third (PC3) for 15.9%. Figure 4 shows the score plots for  
300 PC1 and PC2. These two components clearly separated the four sample groups (Fig. 4).

301 Increasing the culture period increased the PC1 scores, and the biuret group had a smaller PC1  
302 score than the control group. Meanwhile, increasing the culture period decreased the PC2  
303 scores, and the biuret treatment enhanced this decrease. These results suggest that most of the  
304 PC1 variability is explained by a growth component and for PC2 by an aging component.

305 We then compared the mean peak intensities between the control and biuret groups. Excluding  
306 one peak that was considered an artifact due to the assignment of different peak ids to the same

307 compound in different samples, 38 peaks showed significantly different intensities between the  
308 two groups (Fig. 5).  
309 Only two of these peaks, id 310 and id 326, matched the standard compounds. They were  
310 identified as citrulline and citrulline-related compounds, indicating that citrulline, a non-protein  
311 amino acid, accumulated in the biuret-treated rice suspension cells (Fig. 5).  
312 Additionally, the intensity of the peak id 1202 showed a marked increase in biuret-treated cells  
313 (Fig. 5). There were two possible formulas,  $C_{14}H_{20}N_6O_5S_1$  and  $C_{21}H_{20}O_7$ , for the observed m/z  
314 value of this peak. A peak, id 1240, was eluted at nearly the same retention time as 1202, with  
315 less intensity and 2.00 greater m/z value. Presence of the peak supported the former formula  
316 containing a sulfur with major stable isotopes,  $^{32}S$  and  $^{34}S$ . Therefore, it was shown that  
317  $C_{14}H_{20}N_6O_5S_1$ , *S*-adenosyl homocysteine (SAH), was highly accumulated in biuret-treated cells.  
318 SAH is a byproduct of methylation reactions using *S*-adenosylmethionine as a methyl donor and  
319 is a potential competitive inhibitor of methylation reactions. SAH is associated with DNA  
320 hypomethylation (Huang et al., 2019; Rocha et al., 2005). Thus, the accumulation of SAH  
321 observed here could be related to the upregulation of genes in rice suspension cells under biuret  
322 toxicity (Ochiai et al., 2020).  
323 No peaks that could be attributed to allantoin were detected in this analysis.

324

### 325 **Free amino acids accumulation in rice seedlings**

326 The accumulation of allantoin in intact plants and citrulline in cultured cells led us to consider  
327 the possibility that the reduced utilization of assimilated-N occurred before the accumulation of  
328 these N-containing compounds. Therefore, we measured free amino acids in rice seedlings. The  
329 free amino acids concentration in the roots of 8-day-old rice plants grown with 0.3 mmol biuret  
330 was slightly increased compared to the control, but this difference was not significant. The

331 shoot amino acids concentration was significantly increased in the biuret-treated sample (Fig.  
332 6a). The shoot allantoin concentration in these plant samples was also significantly increased by  
333 the biuret treatment, consistent with other trials (Fig. 6b).

334

### 335 **Discussion**

336 In our previous study, we showed that rice plants overexpressing microbial *biuret hydrolase*  
337 were more tolerant to biuret than wild-type plants. Also, the <sup>15</sup>N-biuret uptake rate of the *biuret*  
338 *hydrolase*-overexpressing plants was greater than that of wild-type plants (Ochiai et al., 2020).

339 In this study, we quantified biuret in plants and showed that biuret was not detected in *biuret*  
340 *hydrolase*-overexpressing plants grown with 0.3 mmol L<sup>-1</sup> biuret (Fig. 1e). In contrast, wild-type  
341 rice plants accumulated significant amounts of biuret under the same condition (Fig. 1b). The  
342 results indicate that the *biuret hydrolase*-overexpressing rice plants hydrolyze most of the taken-  
343 up biuret. Thus, the accumulation of biuret in plants is the cause of biuret injury. Supposing a  
344 uniform distribution of biuret in tissue water, the shoot biuret concentration in wild-type rice  
345 seedlings grown with 0.1 and 0.3 mmol L<sup>-1</sup> biuret was estimated to be 0.5 and 1.8 mmol L<sup>-1</sup>,  
346 respectively. Combined with minor injury in rice plants fed with 0.1 mmol L<sup>-1</sup> biuret, a  
347 concentration of biuret in plants on the order of sub-millimolar is seemingly needed to cause  
348 injury. The severity of biuret toxicity in wild-type plants varied among trials, even when the  
349 biuret concentration in plants was nearly the same (Fig. 1, a and d), suggesting the presence of  
350 factors that enhance or alleviate biuret injury.

351 We hypothesized that biuret might specifically inhibit the metabolism of ureide compounds  
352 having structural similarity with biuret. Biuret in the culture solution increased allantoin  
353 concentration in rice shoots (Fig. 1, c and f), but our assumption was not supported as biuret did  
354 not inhibit ALN activity of the crude extract (Fig. 2).



355 Allantoin accumulation has been reported in plants under several environmental stresses  
356 (Casartelli et al., 2019; Kaur et al., 2021; Lescano et al., 2016; Nourimand and Todd, 2016;  
357 Watanabe et al., 2014). Allantoin alleviates reduced plant growth under environmental stress by  
358 activating abscisic acid metabolism (Watanabe et al., 2014) or by enhancing the activity of  
359 antioxidant enzymes (Nourimand and Todd, 2016). In plants under environmental stress,  
360 downregulation of the expression of *ALN* has been reported as a mechanism of allantoin  
361 accumulation (Casartelli et al., 2019; Irani and Todd, 2016; Lescano et al., 2016). The reduced  
362 expression of *OsALN* in roots and *OsAAH* in roots and shoots of the biuret-treated plants at  
363 some time points suggests that degradation suppression contributes to allantoin accumulation in  
364 biuret-injured rice plants (Fig. 3, d and e); however, the expression level of *OsALN* in rice  
365 shoots did not differ between the control and 0.3 mmol L<sup>-1</sup> biuret-treated conditions (Fig. 3d). It  
366 is controversial whether biuret toxicity results in the suppression of *OsALN* because the  
367 expression of *OsALN* was significantly suppressed by biuret in one of the three independent  
368 trials performed in this study (Supplemental Fig. S3). We assume that biuret injury may have  
369 been enhanced by some unknown factors in the trial, resulting in the significant suppression of  
370 *OsALN* expression in shoots. Additionally, *OsALN* expression was lower in roots than in shoots  
371 (Fig. 3d), which is consistent with findings of greater allantoin concentration in roots than in  
372 shoots (Fig. 1, c and f, Fig. 6b), suggesting the contribution of *OsALN* expression regulation in  
373 controlling allantoin accumulation in the tissues. At the same time, however, our results show  
374 that the accumulation of allantoin in rice shoots under biuret toxicity can occur without  
375 significant suppression of *OsALN* in shoots.

376 Biuret altered the expressions of *OsUPS1* and *OsUPS2* (Fig. 3, e and f). *OsUPS1* is a putative  
377 allantoin transporter gene. It is a homolog of the Arabidopsis *AtUPS1* which encodes an  
378 allantoin transporter (Desimone et al., 2002). In contrast to *AtUPS1*, which is up-regulated

379 under N deficiency (Desimone et al., 2002), *OsUPS1* expression is down-regulated under N  
380 deficiency (Lee et al., 2018). *OsUPS1* is supposedly related to the long-distance transport of  
381 allantoin because it is localized to the plasma membrane and is expressed around vascular  
382 tissues (Redillas et al., 2019). Allantoin accumulation in shoots can be caused by altered  
383 translocation of allantoin between the roots and shoots. Since the expression of *OsUPS1* was  
384 increased in shoots under biuret toxicity, an increase in the unloading of allantoin from xylem  
385 vessels in shoots might have resulted in the observed increase in shoot allantoin concentration.  
386 Alternatively, this may indicate increased allantoin transport within shoot cells or from shoots to  
387 roots. The total-N concentration in the shoots of wild-type rice did not differ among biuret  
388 treatments, suggesting that allantoin accumulation in biuret-injured rice plants was a  
389 modification of the form of N within shoots. The shoot allantoin-N as a percentage of shoot  
390 total-N was 0.45% and 0.42% in plants under 0 and 0.1 mmol L<sup>-1</sup> biuret treatment, whereas it  
391 increased to 0.71% in plants under 0.3 mmol L<sup>-1</sup> biuret treatment. Furthermore, the expression  
392 of *OsUPS1* was higher in roots where allantoin was more abundant than in shoots under control  
393 conditions (Fig. 1c, Fig. 3h). In *Arabidopsis* roots, *AtUPS5L* localizes to endoplasmic reticulum  
394 and trans-Golgi network/early endosome, in addition to the plasma membrane, and *AtUPS5*  
395 may be involved in the vesicular export of allantoin under stress (Lescano et al., 2020a).  
396 Although *OsUPS1* has been shown to localize to the plasma membrane (Redillas et al., 2019), if  
397 it is also localized to organelle membranes, increased allantoin accumulation may lead to more  
398 active transport between organelles or vesicular export in rice shoots under biuret toxicity.  
399 *OsUPS2* has not been characterized; thus, the significance of the change in its expression is  
400 currently unclear. The differentially regulated expression of *OsUPS1* and *OsUPS2* in biuret-  
401 injured rice plants showed that these two homologs play different roles in rice plants.

402 Metabolome analysis showed citrulline accumulation in the rice suspension cells treated with  
403 biuret (Fig. 5). Citrulline is a non-protein amino acid involved in the arginine synthesis  
404 pathway. It is synthesized from ornithine and carbamoyl phosphate. Similar to allantoin,  
405 citrulline is involved in plant stress responses. It has been reported that wild watermelon  
406 (*Citrullus lanatus*), native to deserts, and commercial watermelon plants substantially  
407 accumulate citrulline under drought stress (Kawasaki et al., 2000; Song et al., 2020).  
408 Arabidopsis plants under low CO<sub>2</sub> conditions also accumulate citrulline (Blume et al., 2019).  
409 Citrulline is considered to be a scavenger of hydroxyl radicals (Akashi et al., 2001) or NH<sub>4</sub><sup>+</sup>  
410 (Blume et al., 2019; Joshi and Fernie, 2017) generated under such environmental stresses.  
411 In addition to their importance in the stress response, allantoin and citrulline are N-rich  
412 compounds. Allantoin and allantoic acid are the major forms of N transported from the roots to  
413 the shoots in legumes (Schubert et al., 1986). Allantoin accumulation in Arabidopsis plants is  
414 also induced by a low carbon to N ratio and NH<sub>4</sub><sup>+</sup>-N in the culture medium (Lescano et al.,  
415 2020b). Similarly, citrulline contains three N per molecule and is considered an endogenous  
416 source of N in plants (Ludwig, 1993). The accumulation level of citrulline varies with N  
417 nutritional status in watermelon plants (Song et al., 2020) and is higher in NH<sub>4</sub><sup>+</sup>-fed tobacco  
418 plants than in NO<sub>3</sub><sup>-</sup>-fed plants (Gupta et al., 2013). It is, of course, possible that intact rice and  
419 cultured cells responded differently to biuret, but it is also possible that the accumulation of  
420 these compounds was caused by an imbalance in N metabolism due to biuret injury.  
421 Our results also revealed that the free amino acid concentration markedly increased in rice  
422 shoots under biuret toxicity (Fig. 6a). This result is consistent with previous studies showing  
423 that biuret inhibits the incorporation of amino acids into proteins (Ogata and Yamamoto, 1959;  
424 Webster et al., 1957) and other amino acids accumulate along with citrulline in watermelon  
425 plants under drought stress (Song et al., 2020).

426 Additionally, the free amino acids measurement suggests that allantoin acts as a temporary pool  
427 of taken-up N in the roots, even in the control plants. Given that the amino acids in rice roots are  
428 predominantly glutamine (Ogasawara et al., 2021), there were approximately 200  $\mu\text{mol g}^{-1}$  dw  
429 of amino acid-N and 80  $\mu\text{mol g}^{-1}$  dw of allantoin-N in roots (Fig. 6). In shoots, on the other  
430 hand, N transported from roots as glutamine would be incorporated into proteins and would  
431 accumulate less as allantoin under control conditions. When biuret was supplied to the culture  
432 solution, protein synthesis was inhibited for direct or indirect reasons (Ogata and Yamamoto,  
433 1959; Webster et al., 1957), increasing free amino acids and leading to an increase in allantoin.  
434 Since the de novo purine synthesis from glutamine is a complex process requiring energy input,  
435 and therefore, it is unclear whether accumulation of allantoin occurred via increasing de novo  
436 purine synthesis. Allantoin accumulation could also result from the degradation of existing  
437 purine bases. However, the accumulation of amino acids suggests a surplus of reduced N in rice  
438 plants under biuret toxicity. Glutamine and allantoin may trigger the downregulation of  
439 allantoin degradation, thereby inhibiting the generation of excess  $\text{NH}_4^+$  and maintaining reduced  
440 N in a safer form.

441 In conclusion, we investigated changes in metabolites in rice plants under biuret toxicity to  
442 understand the mechanism of toxicity and found the accumulation of two N-rich compounds,  
443 allantoin in intact rice seedlings and citrulline in suspension-cultured cells. A surplus of amino  
444 acids appeared to occur prior to the accumulation of allantoin. Our results suggest that rice  
445 plants subjected to biuret toxicity need to maintain reduced N in secure forms and prevent the  
446 generation of  $\text{NH}_4^+$ . We are currently conducting experiments to investigate the effect of  
447 different N supply levels and sources on biuret injury in rice plants to clarify the significance of  
448 accumulating these N-rich compounds under biuret toxicity.

449

450 **Acknowledgment**

451 We thank Ms. Megumi Nishii for preparing the rice cell samples used in metabolome analysis.

452 This work was supported in part by JSPS KAKENHI (Grant Number JP19K05755).

453

454 **References**

455

456 Akashi K, Miyake C, Yokota A (2001) Citrulline, a novel compatible solute in drought-tolerant  
457 wild watermelon leaves, is an efficient hydroxyl radical scavenger. *FEBS Lett* 508:438–442.

458 [https://doi.org/10.1016/s0014-5793\(01\)03123-4](https://doi.org/10.1016/s0014-5793(01)03123-4)

459 Aukema KG, Tassoulas LJ, Robinson SL, Konopatski JF, Bygd MD, Wackett LP (2020) Cyanuric  
460 acid biodegradation via biuret: physiology, taxonomy, and geospatial distribution. *Appl*

461 *Environ Microbiol* 86:e01964-19. <https://doi.org/10.1128/AEM.01964-19>

462 Baba A, Hasezawa S, Syono K (1986) Cultivation of rice protoplasts and their transformation  
463 mediated by *Agrobacterium* spheroplasts. *Plant Cell Physiol* 27:463–471.

464 <https://doi.org/10.1093/oxfordjournals.pcp.a077122>

465 Blume C, Ost J, Mühlenbruch M, Peterhänsel C, Laxa M (2019) Low CO<sub>2</sub> induces urea cycle  
466 intermediate accumulation in *Arabidopsis thaliana*. *PloS One* 14:e0210342.

467 <https://doi.org/10.1371/journal.pone.0210342>

468 Caldana C, Scheible WR, Mueller-Roeber B, Ruzicic S (2007) A quantitative RT-PCR platform  
469 for high-throughput expression profiling of 2500 rice transcription factors. *Plant Method*, 3:7.

470 <https://doi.org/10.1186/1746-4811-3-7>

471 Cameron SM, Durchschein K, Richman JE, Sadowsky MJ, Wackett LP (2011) A new family of  
472 biuret hydrolases involved in *S*-triazine ring metabolism. *ACS Catal* 2011:1075–1082.

473 <https://doi.org/10.1021/cs200295n>

474 Casartelli A, Melino VJ, Baumann U, Riboni M, Suchecki R, Jayasinghe NS, Mendis H,  
475 Watanabe M, Erban A, Zuther E, Hoefgen R, Roessner U, Okamoto M, Heuer S (2019)

476 Opposite fates of the purine metabolite allantoin under water and nitrogen limitations in bread

477 wheat. *Plant Mol Biol* 99:477–497. <https://doi.org/10.1007/s11103-019-00831-z>

478 Collier R, Tegeder M (2012) Soybean ureide transporters play a critical role in nodule  
479 development, function and nitrogen export. *Plant J* 72:355–367. <https://doi.org/10.1111/j.1365->  
480 313X.2012.05086.x

481 Desimone M, Catoni E, Ludewig U, Hilpert M, Schneider A, Kunze R, Tegeder M, Frommer W  
482 B, Schumacher K (2002) A novel superfamily of transporters for allantoin and other oxo  
483 derivatives of nitrogen heterocyclic compounds in *Arabidopsis*. *Plant Cell* 14:847–856.  
484 <https://doi.org/10.1105/tpc.010458>

485 Duran VA, Todd CD (2012) Four allantoinase genes are expressed in nitrogen-fixing soybean.  
486 *Plant Physiol Biochem* 54:149–155. <https://doi.org/10.1016/j.plaphy.2012.03.002>

487 Esquirol L, Peat TS, Wilding M, Lucent D, French NG, Hartley CJ, Newman J, Scott C (2018)  
488 Structural and biochemical characterization of the biuret hydrolase (BiuH) from the cyanuric  
489 acid catabolism pathway of *Rhizobium leguminosorum* bv. *viciae* 3841. *PLoS One*  
490 13:e0192736. <https://doi.org/10.1371/journal.pone.0192736>

491 Gupta KJ, Brotman Y, Segu S, Zeier T, Zeier J, Persijn ST, Cristescu SM, Harren FJ, Bauwe H,  
492 Fernie AR, Kaiser WM, Mur LA (2013) The form of nitrogen nutrition affects resistance  
493 against *Pseudomonas syringae* pv. *phaseolicola* in tobacco. *J Exp Bot*, 64:553–568.  
494 <https://doi.org/10.1093/jxb/ers348>

495 Hewitt EJ (1966) The composition of the nutrient solution. In: Hewitt EJ (ed) *Sand and water*  
496 *culture methods used in the study of plant nutrition*. Farnham Royal Bucks, Commonwealth  
497 Agricultural Bureaux, Slough, pp 190.

498 Huang XY, Li M, Luo R, Zhao FJ, Salt DE (2019) Epigenetic regulation of sulfur homeostasis in  
499 plants. *J Exp Bot* 70:4171–4182. <https://doi.org/10.1093/jxb/erz218>

500 Irani S, Todd CD (2016) Ureide metabolism under abiotic stress in *Arabidopsis thaliana*. *J Plant*  
501 *Physiology* 199:87–95. <https://doi.org/10.1016/j.jplph.2016.05.011>

502 Joshi V, Fernie AR (2017) Citrulline metabolism in plants. *Amino Acids* 49:1543–1559.  
503 <https://doi.org/10.1007/s00726-017-2468-4>

504 Kaur H, Chowrasia S, Gaur VS, Mondal TK (2021) Allantoin: Emerging role in plant abiotic  
505 stress tolerance. *Plant Mol Biol Report* 39:648–661. [https://doi.org/10.1007/s11105-021-](https://doi.org/10.1007/s11105-021-01280-z)  
506 [01280-z](https://doi.org/10.1007/s11105-021-01280-z)

507 Kawasaki S, Miyake C, Kohchi T, Fujii S, Uchida M, Yokota A (2000) Responses of wild  
508 watermelon to drought stress: accumulation of an ArgE homologue and citrulline in leaves  
509 during water deficits. *Plant Cell Physiol* 41:864–873. <https://doi.org/10.1093/pcp/pcd005>

510 Lee DK, Redillas M, Jung H, Choi S, Kim YS, Kim JK (2018) A nitrogen molecular sensing  
511 system, comprised of the ALLANTOINASE and UREIDE PERMEASE 1 genes, can be used  
512 to monitor N status in rice. *Front Plant Sci* 9:444. <https://doi.org/10.3389/fpls.2018.00444>

513 Lescano I, Bogino MF, Martini C, Tessi TM, González CA, Schumacher K, Desimone M. (2020a)  
514 Ureide permease 5 (atups5) connects cell compartments involved in ureide metabolism. *Plant*  
515 *Physiol*, 182:1310–1325. <https://doi.org/10.1104/pp.19.01136>

516 Lescano CI, Martini C, González CA, Desimone M (2016) Allantoin accumulation mediated by  
517 allantoinase downregulation and transport by Ureide Permease 5 confers salt stress tolerance  
518 to Arabidopsis plants. *Plant Mol Biol* 91:581–595. <https://doi.org/10.1007/s11103-016-0490-7>

519 Lescano I, Devegili AM, Martini C, Tessi TM, González CA, Desimone M (2020b) Ureide  
520 metabolism in *Arabidopsis thaliana* is modulated by C:N balance. *J Plant Res* 133:739–749.  
521 <https://doi.org/10.1007/s10265-020-01215-x>

522 Ludwig RA (1993) Arabidopsis chloroplasts dissimilate L-arginine and L-citrulline for use as N  
523 source. *Plant Physiol* 101:429–434. <https://doi.org/10.1104/pp.101.2.429>

524 Mikkelsen RL (1990) Biuret in urea fertilizer. *Fertilizer Res* 26: 311-318



525 Moore S, Stein WH (1954). A modified ninhydrin reagent for the photometric determination of  
526 amino acids and related compounds. *J Biol Chem*, 211:907–913.

527 Nourimand M, Todd CD (2016) Allantoin increases cadmium tolerance in *Arabidopsis* via  
528 activation of antioxidant mechanisms. *Plant Cell Physiol* 57:2485–2496.  
529 <https://doi.org/10.1093/pcp/pcw162>

530 Ochiai K, Uesugi A, Masuda Y, Nishii M, Matoh T (2020) Overexpression of exogenous *biuret*  
531 *hydrolase* in rice plants confers tolerance to biuret toxicity. *Plant Direct* 4:e00290.  
532 <https://doi.org/10.1002/pld3.290>

533 Ogasawara S, Ezaki M, Ishida R, Sueyoshi K, Saito S, Hiradate Y, Kudo T, Obara M, Kojima S,  
534 Uozumi N, Tanemura K, Hayakawa T (2021) Rice amino acid transporter-like 6 (OsATL6) is  
535 involved in amino acid homeostasis by modulating the vacuolar storage of glutamine in roots.  
536 *Plant J* 107:1616–1630. <https://doi.org/10.1111/tpj.15403>

537 Ogata T, Yamamoto M (1959) Effects of biuret on the metabolism of germinating plant. I. *Jpn J*  
538 *Soil Sci Plant Nutr* 29:549-555 (*in Japanese*)

539 Pang Z, Chong J, Zhou G, de Lima Morais DA, Chang L, Barrette M, Gauthier C, Jacques PÉ, Li  
540 S, Xia J (2021) MetaboAnalyst 5.0: narrowing the gap between raw spectra and functional  
541 insights. *Nucleic Acids Res* 49:W388–W396. <https://doi.org/10.1093/nar/gkab382>

542 Redillas M, Bang SW, Lee DK, Kim YS, Jung H, Chung PJ, Suh JW, Kim JK (2019) Allantoin  
543 accumulation through overexpression of *ureide permease 1* improves rice growth under limited  
544 nitrogen conditions. *Plant Biotechnol J* 17:1289–1301. <https://doi.org/10.1111/pbi.13054>

545 Robinson SL, Badalamenti JP, Dodge AG, Tassoulas LJ, Wackett LP (2018) Microbial  
546 biodegradation of biuret: defining biuret hydrolases within the isochorismatase superfamily.  
547 *Environ microbiol* 20:2099–2111. <https://doi.org/10.1111/1462-2920.14094>

548 Rocha PS, Sheikh M, Melchiorre R, Fagard M, Boutet S, Loach R, Moffatt B, Wagner C,  
549 Vaucheret H, Furner I (2005) The Arabidopsis HOMOLOGY-DEPENDENT GENE  
550 SILENCING1 gene codes for an *S*-adenosyl-L-homocysteine hydrolase required for DNA  
551 methylation-dependent gene silencing. *Plant Cell* 17:404–417.  
552 <https://doi.org/10.1105/tpc.104.028332>

553 Sakurai N, Ara T, Enomoto M, Motegi T, Morishita Y, Kurabayashi A, Iijima Y, Ogata Y,  
554 Nakajima D, Suzuki H, Shibata D (2014) Tools and databases of the KOMICS web portal for  
555 preprocessing, mining, and dissemination of metabolomics data. *BioMed Res Int* 2014:194812.  
556 <https://doi.org/10.1155/2014/194812>

557 Schubert KR (1986) Products of biological nitrogen fixation in higher plants: Synthesis, transport,  
558 and metabolism. *Annu Rev Plant Physiol* 37:539–574.  
559 <https://doi.org/10.1146/annurev.pp.37.060186.002543>

560 Soltabayeva A, Srivastava S, Kurmanbayeva A, Bekturova A, Fluhr R, Sagi M (2018) Early  
561 senescence in older leaves of low nitrate-grown *atxdh1* uncovers a role for purine catabolism  
562 in n supply. *Plant Physiol* 178:1027–1044. <https://doi.org/10.1104/pp.18.00795>

563 Song Q, Joshi M, DiPiazza J, Joshi V (2020). Functional relevance of citrulline in the vegetative  
564 tissues of watermelon during abiotic stresses. *Front Plant Sci*, 11:512.  
565 <https://doi.org/10.3389/fpls.2020.00512>

566 Watanabe S, Matsumoto M, Hakomori Y, Takagi H, Shimada H, Sakamoto A (2014) The purine  
567 metabolite allantoin enhances abiotic stress tolerance through synergistic activation of abscisic  
568 acid metabolism. *Plant Cell Environ* 37:1022–1036. <https://doi.org/10.1111/pce.12218>

569 Webster GC, Berner RA, Gansa AN (1957) The effect of biuret on protein synthesis in plants.  
570 *Plant Physiol* 32:60–61. <https://doi.org/10.1104/pp.32.1.60>

571 Yamaji N, Ma JF (2009) A transporter at the node responsible for intervascular transfer of silicon  
572 in rice. *Plant Cell* 21:2878–2883. <https://doi.org/10.1105/tpc.109.069831>  
573 Young EZ, Conway CF (1942) On the estimation of allantoin by the riminischryver reaction. *J*  
574 *Biol Chem* 142:839-853. [https://doi.org/10.1016/S0021-9258\(18\)45082-X](https://doi.org/10.1016/S0021-9258(18)45082-X)  
575

576 **Statements and Declarations**

577 **Funding:** This work was supported in part by JSPS KAKENHI Grant Number JP19K05755.

578

579 **Competing interests:** The authors have no relevant financial or non-financial interests to  
580 disclose.

581

582 **Author contributions:** Kumiko Ochiai and Toru Matoh conceived and designed the research.  
583 Kumiko Ochiai and Yosuke Nomura performed experiments and analyzed the data. Asuka  
584 Uesugi generated *biuret hydrolase*-overexpressing rice lines. Kumiko Ochiai wrote the  
585 manuscript with input from other authors.

586

587 **Data availability:** the data supporting the findings of this study are available within the article  
588 and its supplementary materials.

589

590

591 **Figure legend**

592 **Fig. 1** Effects of biuret on dry weight (a, d), biuret concentration (b, e), and allantoin concentration  
593 (c, f) in roots and shoots of 7-day-old wild-type rice plants (a–c) and 9-day-old *biuret hydrolase*-  
594 overexpressing rice lines (d–f). Bars and circles represent mean and each sample, respectively.  
595 nd means not detected. (a–c) Wild-type plants were grown with 0, 0.1, and 0.3 mmol L<sup>-1</sup> biuret  
596 supplemented in the culture solution. Ten seedlings were combined for a single sample. Different  
597 alphabets indicate significant difference among treatments in each organ ( $p < 0.05$ , Tukey's test,  
598  $n = 3$ ). (d–f) Wild-type and two independent transgenic lines (B3-9-1 and B2-3-3) were grown  
599 with or without 0.3 mmol L<sup>-1</sup> biuret in the culture solution. Four to six plants were combined into  
600 one sample. Gray and black bars represent control and biuret-treated plants, respectively.  
601 Asterisks indicate significant difference between the treatment ( $*p < 0.05$ ;  $**p < 0.01$ , Welch's t-  
602 test,  $n = 3$ ). Different alphabets indicate significant difference in each organ ( $p < 0.05$ , Tukey's  
603 test,  $n = 3$ ).

604

605 **Fig. 2** Inhibitory effect of biuret for allantoinase activity. Crude extracts were prepared from  
606 shoots of 9-day-old rice seedlings hydroponically grown without biuret. Extracts were incubated  
607 at 30°C with 10 mmol L<sup>-1</sup> allantoin, 50 mmol L<sup>-1</sup> Tricine-NaOH (pH8.0), 2mmol L<sup>-1</sup> MnSO<sub>4</sub>, and  
608 the desired concentration of biuret for 30min. The amount of allantoic acid produced from  
609 allantoin was colorimetrically determined. Same shape symbols indicate a same crude extract.  
610 Crossbars represent the mean value. The means were not significantly different among treatments  
611 at 5% level (One-way ANOVA with blocking,  $n = 4$ ).

612

613 **Fig. 3** Relative expression of genes related to purine degradation and ureide metabolisms in roots  
614 and shoots of 4 to 7-day old rice seedlings. Rice plants were hydroponically grown under the  
615 control condition and 0.3 mmol L<sup>-1</sup> biuret toxicity. Data obtained from two independent trials,

616 each with three replicates, are combined and shown. The relative expression levels of *OsXO* (a),  
617 *OsUO* (b), *OsALNS* (c), *OsALN* (d), *OsAAH* (e), *OsUGlyAH* (f), *OsUAH* (g), *OsUPS1* (h),  
618 *OsUPS2* (i), and *OsUPS3* (j). The expression levels were normalized to the expression of  
619 *Ubiquitin* and *Actin1* and expressed in log<sub>2</sub> scale. Gray and black symbols indicate control and  
620 biuret treated samples, respectively. Crossbars indicate means of the six samples. Asterisks  
621 indicate statistically significant difference between the treatments at the time point. \* $p < 0.05$ ;  
622 \*\* $p < 0.01$ ; \*\*\* $p < 0.001$  (n = 6, Welch's t-test). Numerical values above asterisks indicate log<sub>2</sub>  
623 fold-change relative to the control plants.

624

625 **Fig. 4** Principal component analysis of metabolomics profile of control and biuret-treated rice  
626 suspension cells. Rice cells were transferred into a medium without biuret or with 0.3 mmol L<sup>-1</sup>  
627 biuret and harvested 3 and 5 days after transfer. Closed symbols indicate control cells, and open  
628 symbols indicate biuret-treated cells. Circles indicate day 3 samples, and triangles indicate day 5  
629 samples.

630

631 **Fig. 5** Normalized peak intensities of differentially accumulated metabolites between control and  
632 biuret treated rice suspension cells. Peaks with significantly different intensity between the  
633 control-group and biuret-group are shown in the list ( $p < 0.05$ , Welch's t-test, n = 4). RT column  
634 indicate retention time in second. In the formula column, the formula is shown when the formula  
635 is uniquely determined from the m/z value, blank when there are multiple possible candidates,  
636 and unknown when there are no candidates. D3C: day 3 control cell sample; D3B: day 3 biuret-  
637 treated cell sample; D5C: day 5 control cell sample; D5B: day 5 biuret-treated cell sample.

638

639 **Fig. 6** Free amino acids concentration (a) and allantoin concentration (b) in 8-day-old seedlings.  
640 Rice plants were hydroponically grown under the control condition and 0.3 mmol L<sup>-1</sup> biuret  
641 toxicity. Five plants were combined for a single sample. Boxes indicate the mean of three samples,

642 and symbols indicate each sample. Asterisks indicate a statistically significant difference between  
643 the treatments (Welch's t-test). \*\* $p < 0.01$ ; \*\*\* $p < 0.001$ .  
644

645 **Supplemental Materials**

646 **Supplemental Fig. S1** Allantoin concentration in 9-day-old rice shoots measured by colorimetric  
647 and HPLC-UV. Plants were grown hydroponically under the three biuret treatments. Control:  
648 plants did not receive biuret; NB: plants were grown without biuret for three days after sowing,  
649 and with 0.3 mmol L<sup>-1</sup> biuret supplemented in the culture solution from the fourth day; BN: plants  
650 were grown with 0.3 mmol L<sup>-1</sup> biuret for 6 days after sowing and transferred to new culture  
651 solution without biuret on the seventh day. Fresh shoots of 9-day-old seedlings were ground under  
652 liquid N<sub>2</sub> and extracted with 10-fold volume of distilled water. After centrifugation, the  
653 supernatant was used for allantoin determination. Gray boxes indicate mean allantoin  
654 concentration determined colorimetrically and black boxes indicate that determined by the HPLC  
655 method. Symbols indicate each sample. The statistical significance of the differences between the  
656 methods was determined through paired t-test (n = 2). ns: not significant.

657

658 **Supplemental Fig. S2** Pictures of 9-day-old wild-type rice seedlings and two *biuret hydrolase*-  
659 overexpressing lines. From left to right: wild type and overexpressing lines B3-9-1 and B2-3-3.  
660 Upper: seedlings grown in the control culture solution. Lower: seedlings grown in the culture  
661 solution supplemented with 0.3 mmol L<sup>-1</sup> biuret. Bars show 10 cm.

662

663 **Supplemental Fig. S3** Relative expression levels of (a) *OsALN* and (b) *OsUO* in 3 to 9-day-old  
664 rice shoots in the preliminary experiment. Rice plants were hydroponically grown with or  
665 without 0.3 mmol L<sup>-1</sup> biuret supplied in the culture solution. Measurements were made using  
666 plants grown in an independent trial from those shown in Figure 3. The relative expression  
667 levels were normalized to those of *Ubiquitin* and *Actin1* and expressed on a log<sub>2</sub> scale. Gray  
668 and black squares indicate control and biuret-treated plants, respectively; data represent the



669 mean  $\pm$  SD (n = 4). Asterisks indicate statistically significant differences between treatments at  
670 the time point (Welch's t-test). \* $p$  < 0.05; \*\* $p$  < 0.01; \*\*\* $p$  < 0.001. Numerical values above  
671 asterisks indicate log<sub>2</sub> fold-change relative to the control plants.

672

673 **Supplemental Data S1** Peak intensities in Metabolome analysis.

674

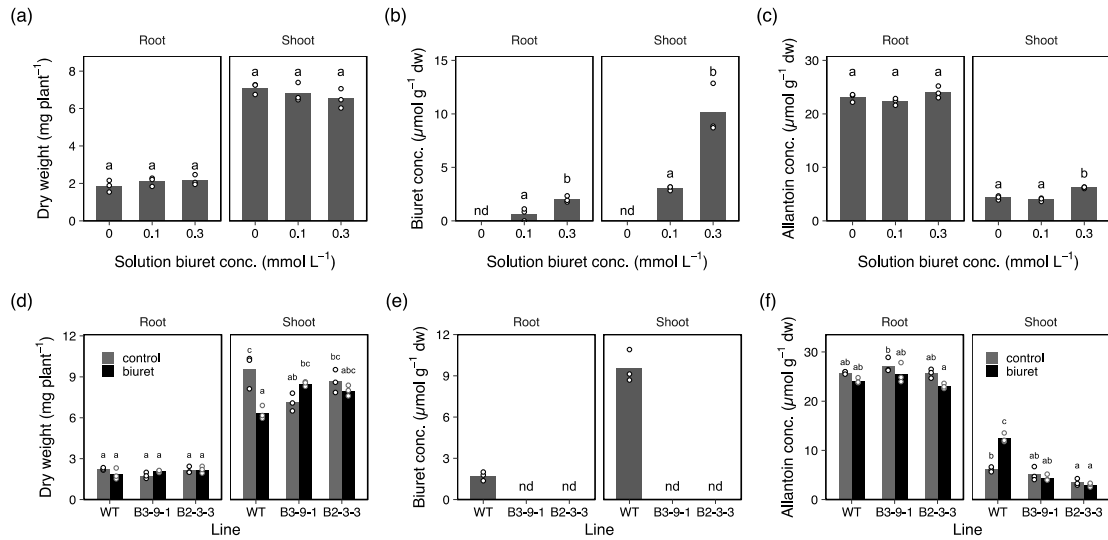


**Fig. 1** Effects of biuret on dry weight (a, d), biuret concentration (b, e), and allantoin concentration (c, f) in roots and shoots of 7-day-old wild-type rice plants (a–c) and 9-day-old *biuret hydrolase*-overexpressing rice lines (d–f). Bars and circles represent mean and each sample, respectively. nd means not detected. (a–c) Wild-type plants were grown with 0, 0.1, and 0.3 mmol L<sup>-1</sup> biuret supplemented in the culture solution. Ten seedlings were combined for a single sample. Different alphabets indicate significant difference among treatments in each organ ( $p < 0.05$ , Tukey's test,  $n = 3$ ). (d–f) Wild-type and two independent transgenic lines (B3-9-1 and B2-3-3) were grown with or without 0.3 mmol L<sup>-1</sup> biuret in the culture solution. Four to six plants were combined into one sample. Gray and black bars represent control and biuret-treated plants, respectively. Asterisks indicate significant difference between the treatment ( $*p < 0.05$ ;  $**p < 0.01$ , Welch's t-test,  $n = 3$ ). Different alphabets indicate significant difference in each organ ( $p < 0.05$ , Tukey's test,  $n = 3$ ).

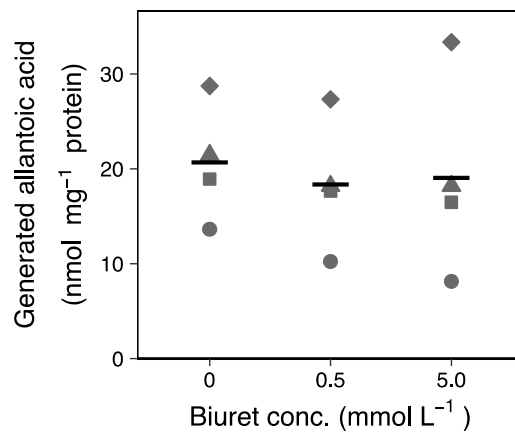


**Fig. 2** Inhibitory effect of biuret for allantoinase activity. Crude extracts were prepared from shoots of 9-day-old rice seedlings hydroponically grown without biuret. Extracts were incubated at 30°C with 10 mmol L<sup>-1</sup> allantoin, 50 mmol L<sup>-1</sup> Tricine-NaOH (pH8.0), 2mmol L<sup>-1</sup> MnSO<sub>4</sub>, and the desired concentration of biuret for 30min. The amount of allantoic acid produced from allantoin was colorimetrically determined. Same shape symbols indicate a same crude extract. Crossbars represent the mean value. The means were not significantly different among treatments at 5% level (One-way ANOVA with blocking, n = 4).

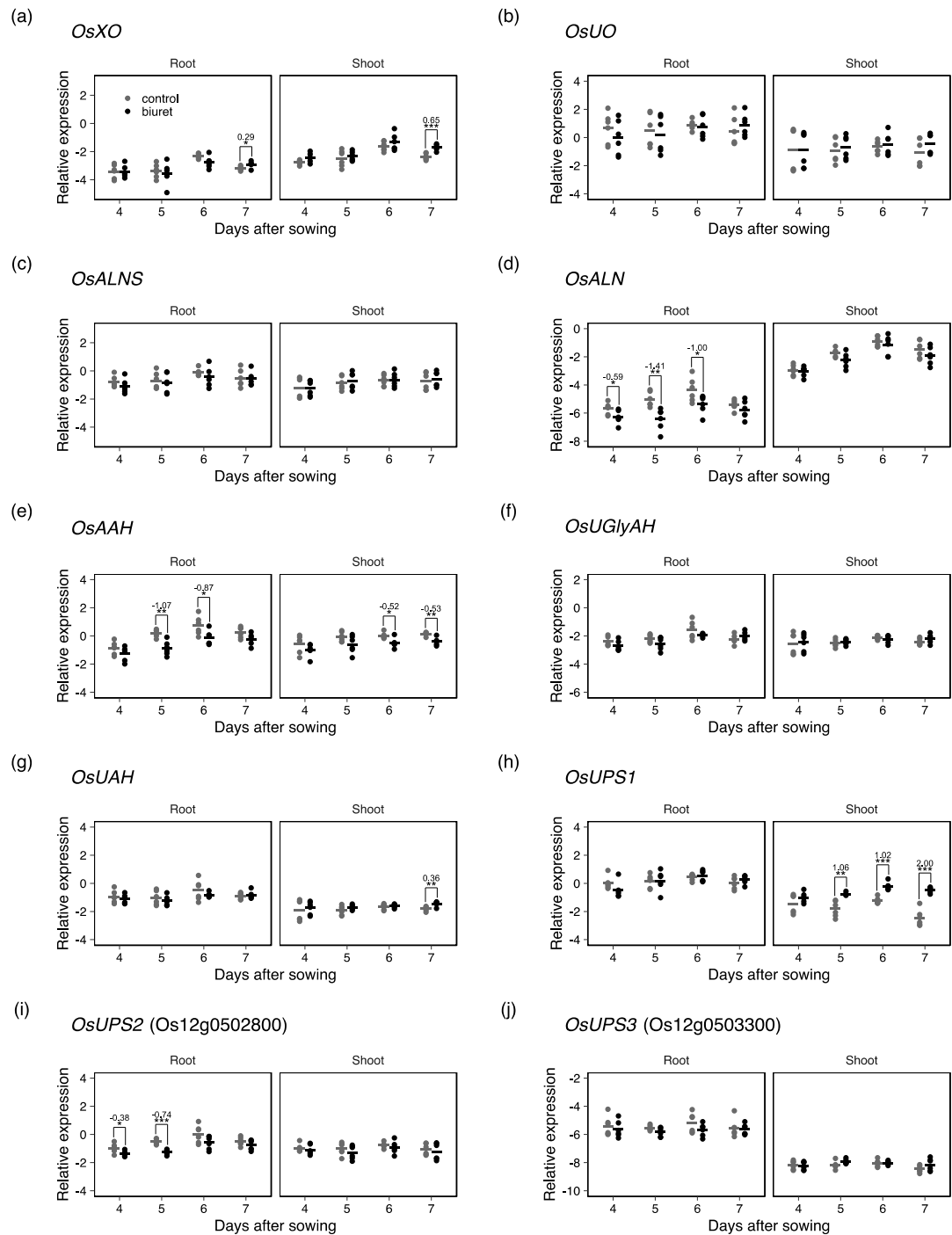


**Fig. 3** Relative expression of genes related to purine degradation and ureide metabolisms in roots and shoots of 4 to 7-day old rice seedlings. Rice plants were hydroponically grown under the control condition and 0.3 mmol L<sup>-1</sup> biuret toxicity. Data obtained from two independent trials,

each with three replicates, are combined and shown. The relative expression levels of *OsXO* (a), *OsUO* (b), *OsALNS* (c), *OsALN* (d), *OsAAH* (e), *OsUGlyAH* (f), *OsUAH* (g), *OsUPS1* (h), *OsUPS2* (i), and *OsUPS3* (j). The expression levels were normalized to the expression of *Ubiquitin* and *Actin1* and expressed in log<sub>2</sub> scale. Gray and black symbols indicate control and biuret treated samples, respectively. Crossbars indicate means of the six samples. Asterisks indicate statistically significant difference between the treatments at the time point. \* $p < 0.05$ ; \*\* $p < 0.01$ ; \*\*\* $p < 0.001$  (n = 6, Welch's t-test). Numerical values above asterisks indicate log<sub>2</sub> fold-change relative to the control plants.

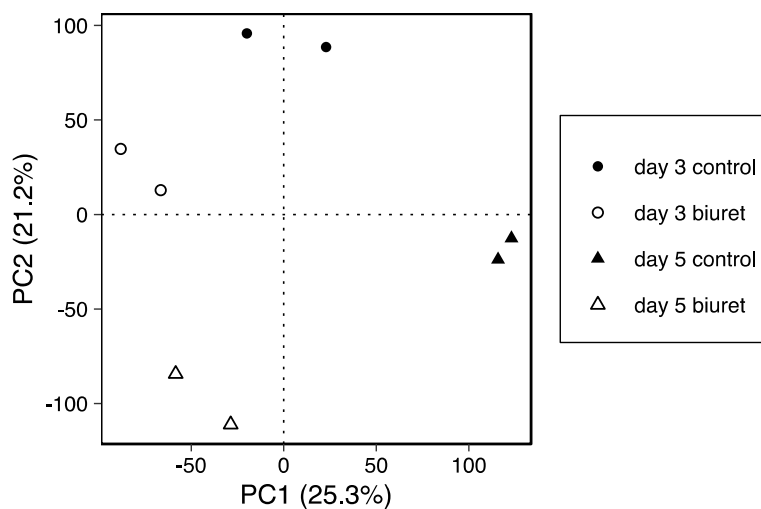


**Fig. 4** Principal component analysis of metabolomics profile of control and biuret-treated rice suspension cells. Rice cells were transferred into a medium without biuret or with  $0.3 \text{ mmol L}^{-1}$  biuret and harvested 3 and 5 days after transfer. Closed symbols indicate control cells, and open symbols indicate biuret-treated cells. Circles indicate day 3 samples, and triangles indicate day 5 samples.

ID	RT (sec)	m/z	Formula	Normalized intensity							
				D3C1	D3C2	D5C1	D5C2	D3B1	D3B2	D5B1	D5B2
47	37	102.0913	C5H11N1O1					3	3	3	4
239	54	170.0576	C4H12N1O4P1					-2	-1	-1	-1
310	55	176.1029	C6H13N3O3	3	3	3	3	5	5	5	5
326	56	159.0763	C6H10N2O3	1	2	1	1	2	3	3	3
342	57	120.0655	C4H9N1O3	2	3	3	1	3	4	3	4
372	58	138.0549	C7H7N1O2	3	4	3	4	3	1	3	2
432	58	268.0848	C9H17N1O6S1					-1	-1	0	0
448	59	385.1288						2	3	3	0
811	80	206.0480	C7H11N1O4S1					1	2	2	3
826	82	236.0585	C11H10N3O1C1					-3	0	1	1
864	83	238.0742	C8H15N1O5S1					-2	0	0	1
1100	99	284.1337	C10H21N1O8					0	1	1	1
1117	102	376.1283						0	2	1	2
1127	103	247.1286	C10H18N2O5					0	0	0	-2
1161	106	163.0599	C6H10O5	0	1	2	0	0	0	0	0
1202	110	385.1287					0	5	7	6	6
1240	114	387.1245						0	2	1	2
1247	114	136.0616	C5H5N5					-3	1	-1	0
1248	114	193.5696	Unknown Peak					1	4	2	4
1251	114	170.0651	Unknown Peak					2	4	2	4
1354	138	296.1160	C14H18N3O2C1	-1				0	-1	0	1
1719	263	529.1268						2	1	1	3
1722	264	190.1072	C8H15N1O4	2	2	3	2	3	3	3	4
1805	278	285.0901						0	1	1	2
1867	292	149.1171	C7H16O3					0	-1	0	0
1954	309	304.1389	C13H21N1O7	1	1	2	2	1	0	1	0
2067	322	229.1545	C11H20N2O3	0				2	-1	2	2
2219	339	352.1389	C17H21N1O7	0	0	1	1				0
2222	339	445.0944						2	3	4	4
2340	360	587.2546		-1				2	1	1	-1
2444	386	293.1164						1	2	1	1
2470	394	159.1014	C8H14O3					0	1	1	2
2476	395	335.1334		2	3	3	3	3	4	5	5
2477	395	370.1706		4	3	4	3	4	5	5	5
2669	487	141.1273	C9H16O1					0	0	1	1
2837	645	1118.7230		1				-3	-3	-2	-2
3022	806	522.3552	C26H52N1O7P1	-1				0	0	1	-2
3183	965	487.3603	Unknown Peak	-1	-1	-1	-1				-2

**Fig. 5** Normalized peak intensities of differentially accumulated metabolites between control and biuret treated rice suspension cells. Peaks with significantly different intensity between the control-group and biuret-group are shown in the list ( $p < 0.05$ , Welch's t-test,  $n = 4$ ). RT column indicate retention time in second. In the formula column, the formula is shown when the formula is uniquely determined from the m/z value, blank when there are multiple possible candidates, and unknown when there are no candidates. D3C: day 3 control cell sample; D3B: day 3 biuret-treated cell sample; D5C: day 5 control cell sample; D5B: day 5 biuret-treated cell sample.

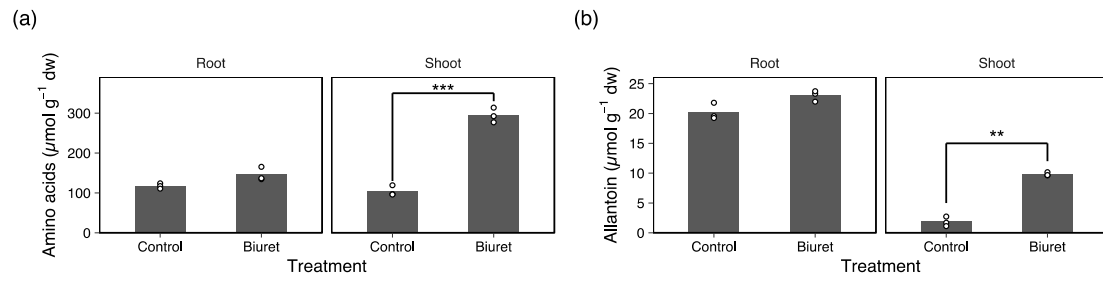


**Fig. 6** Free amino acids concentration (a) and allantoin concentration (b) in 8-day-old seedlings. Rice plants were hydroponically grown under the control condition and 0.3 mmol L<sup>-1</sup> biuret toxicity. Five plants were combined for a single sample. Boxes indicate the mean of three samples, and symbols indicate each sample. Asterisks indicate a statistically significant difference between the treatments (Welch's t-test). \*\* $p < 0.01$ ; \*\*\* $p < 0.001$ .